Proteomic Analysis of Cleavage Events Reveals a Dynamic Two-step Mechanism for Proteolysis of a Key Parasite Adhesive Complex*

Xing W. Zhou‡, Michael J. Blackman§, Steven A. Howell§, and Vern B. Carruthers‡¶

The transmembrane micronemal protein MIC2 and its partner M2AP comprise an adhesive complex that is required for rapid invasion of host cells by the obligate intracellular parasite *Toxoplasma gondii*. Recent studies have shown that the MIC2/M2AP complex undergoes extensive proteolytic processing on the parasite surface during invasion, including primary processing of M2AP by unknown proteases and proteolytic shedding of the complex by an anonymous protease called MPP1. While it was shown that MPP1-mediated cleavage is necessary for efficient invasion, it remained unclear whether the adhesive complex was liberated by juxtamembrane or intramembrane proteolysis. Here, using a three-phase strategy of assigning cleavage sites based on intact matrix-assisted laser desorption/ionization mass followed by confirmation by enzymatic digestion and inhibitor profiling, we demonstrate that M2AP is processed by two parasite-derived proteases called MPP2 and MPP3. We also define the substrate repertoire of MPP2 by two-dimensional differential gel electrophoresis using fluorescent tags. Finally, we use complementary mass spectrometric techniques to unequivocally show that MIC2 is shed by intramembrane cleavage within its anchoring domain. Based on the properties of this cleavage site, we conclude that the sheddase, MPP1, is likely a multipass membrane protease of the Rhomboid family. Our data support a novel two-step proteolysis model that includes primary processing of the MIC2/M2AP complex followed by secondary cleavage to shed the complex from the parasite surface during the final steps of invasion. ***Molecular & Cellular Proteomics 3:565–576, 2004.***

The protozoan parasite *Toxoplasma gondii* is an intracellular pathogen classified in the phylum Apicomplexa. Infection with *T. gondii* causes severe illness (toxoplasmosis) when the pathogen is contracted congenitally or when it is reactivated in immune-suppressed individuals (1). Despite the usually effective antibiotics available for toxoplasmosis, undesired side effects of these drugs complicate current treatments. Recent studies have revealed that proteolytic processing plays crucial roles in parasite survival (reviewed in Ref. 2), and inhibition of proteases by selective inhibitors has been shown to block *Toxoplasma* invasion and intracellular development (3, 4). Accordingly, new insight into the proteolytic events in *T. gondii* has the potential to lead to the development of novel therapeutic strategies. In addition, *T. gondii* has recently gained attention as a model organism for apicomplexan parasites because it shares common apical structures and a similar mechanism of active invasion with relatives such as the malaria parasite *Plasmodium*, but is genetically easier to manipulate (5).

One of the first events in *T. gondii* invasion, coincident with apical attachment of the parasite to the host cell, is the release of numerous "soluble" and transmembrane (TM)[1]-anchored proteins from secretory vesicles called micronemes (6, 7). These micronemal proteins (MICs) contain a variety of conserved adhesive domains, and several have been demonstrated to bind to receptors on mammalian cells (8). MIC2 (9) is a micronemal TM protein consisting of six thrombospondin-

From the ‡W. Harry Feinstone Department of Molecular Microbiology and Immunology, Johns Hopkins Bloomberg School of Public Health, Baltimore, MD 21205; and §Division of Parasitology, National Institute for Medical Research, Mill Hill, London NW7 1AA, United Kingdom

Received, November 20, 2003, and in revised form, February 19, 2004

Published, MCP Papers in Press, February 24, 2004, DOI 10.1074/mcp.M300123-MCP200

[1] The abbreviations used are: TM, transmembrane; MICs, micronemal proteins; M2AP, MIC2-associated protein; mM2AP, mature M2AP; MPP1, Microneme protein protease 1; MPP2, microneme protein protease 2; MPP3, microneme protein protease 3; amu, atomic mass units; ESA, excretory/secretory antigen; DMEM, Dulbecco's modified Eagle's medium; 2DE, two-dimensional gel electrophoresis; MS, mass spectrometry; MALDI, matrix-assisted laser desorption/ionization; ESI, electrospray ionization; TOF, time-of-flight; CID, collision-induced dissociation; CytD, cytochalasin D; ALLN, *N*-acetyl-Leu-Leu-norleucinal; ALLM, *N*-acetyl-Leu-Leu-methioninal; CHAPS, 3-[(3-cholamidopropyl)dimethylammonio]-1-propanesulfonic acid; 2D-DIGE, two-dimensional differential gel electrophoresis; Cy3, 1-(5-carboxypentyl)-1′-propylindocarbocyanine halide *N*-hydroxy-succinimidyl ester; Cy5, 1-(5-carboxypentyl)-1′-methylindodicarbocyanine halide *N*-hydroxysuccinimidyl ester; TFA, trifluoroacetic acid; IPG, immobilized pH gradient; HPLC, high-pressure liquid chromatography; PMSF, phenylmethanesulfonyl fluoride; 1D, one dimensional; DTT, dithiothreitol; PMF, peptide mass fingerprinting; QTOF, quadrupole TOF; RIP, regulated intramembrane proteolysis; JP, juxtamembrane proteolysis; MSP, merozoite surface protein.

© 2004 by The American Society for Biochemistry and Molecular Biology, Inc.
This paper is available on line at http://www.mcponline.org

Downloaded from http://www.mcponline.org/ by guest on September 22, 2019

like adhesive repeats (M-domain), an integrin-like adhesive sequence (A-domain), and a short cytoplasmic tail indirectly connected to the actin-myosin system beneath the plasma membrane of the parasite (10). Within 15 min of synthesis, MIC2 is assembled into a complex with another micronemal protein, M2AP (11). M2AP is composed of a short pro-domain, a β-sheet domain, and a C-terminal coil domain. The complex remains associated during transit through the Golgi complex and storage in the micronemes. Upon parasite attachment to a host cell, the MIC2/M2AP complex is rapidly secreted onto the apical surface of the parasite. As *T. gondii* uses its actin-myosin system to actively penetrate into a target cell (12, 13), the MIC2/M2AP complex is translocated over the parasite body to its posterior end (14), where the ectodomain of MIC2 (A-domain and M-domain) is released through C-terminal proteolysis of MIC2, with M2AP still bound in the complex (15). The observation that discharge and translocation of MIC2/M2AP is tightly correlated with invasion has strongly implied an important role for the complex during invasion (11, 14). This is further supported by recent evidence showing that blocking C-terminal proteolysis of MIC2 can impair host cell entry (16). Together with the observation that M2AP-null mutant parasites are markedly defective in host-cell attachment and invasion (17), the collective evidence strongly suggests that MIC2/M2AP is a key protein complex that is required for efficient invasion. Despite this progress, however, the precise molecular details of how MIC2/M2AP facilitates invasion remain poorly understood.

MIC2 and M2AP undergo extensive proteolytic processing during maturation and invasion (11, 15). Indeed, proteolytic processing is a common post-translational modification for *Toxoplasma* MICs including, for example, AMA1 (18), MIC3 (19), and MIC6 (20). Processing occurs either within the parasite secretory pathway during protein maturation or on the parasite surface during invasion. In the case of M2AP, the pro-domain of M2AP is removed in the Golgi or nascent micronemes. When M2AP is discharged onto the surface of the parasite, it is further truncated into four smaller polypeptides (11). However, the precise cleavage sites and the proteases responsible for the processing remain unknown. Extensive processing of MIC2 also occurs on the parasite surface where this adhesin is multiply cleaved at its N terminus by a parasite-derived protease MPP2 (15). In addition, another parasite-derived protease MPP1 processes MIC2 at an undefined site in its C terminus, releasing the ectodomain into the medium. Recently, the Soldati group (20) demonstrated that a MIC2 hybrid protein containing multiple mutations within its TM anchor was resistant to C-terminal cleavage and shedding. This genetic evidence suggested that C-terminal cleavage might occur within the membrane. However, another recent genetic study by the Sibley group (16) demonstrated that a lysine-containing motif outside the TM segment is necessary for C-terminal processing. Because this C-terminal proteolysis is required for invasion, it is important to address this apparent discrepancy with compelling structural evidence. Also, because MPP1 has not been molecularly cloned or characterized, analysis of its cleavage site specificity could reveal important clues to its enzymatic properties.

Herein we unequivocally demonstrate that MIC2 is liberated from the parasite surface by intramembrane cleavage, based on precise identification of the cleavage site using complementary mass spectrometric approaches. Furthermore, we used proteomic analysis of cleavage sites and protease inhibitor profiling to show that M2AP is multiply processed by MPP2 and at least one additional novel parasite-derived protease we term MPP3. Based on these new findings, we propose a detailed two-step model for the dynamic processing of MIC2/M2AP, which includes primary and secondary processing steps that culminate in shedding of the adhesive complex from the parasite surface.

EXPERIMENTAL PROCEDURES

Materials—Porcine trypsin (sequencing grade) was obtained from Promega (Madison, WI), and endoproteinase Asp-N (excision grade) was obtained either from Calbiochem (La Jolla, CA) or Roche (Indianapolis, IN). ^{18}O water was purchased from Isotec (CK Gas Products Ltd., Hampshire, United Kingdom). Mass spectrometry (MS) calibration mixture II (peptide mass standard kit) was obtained from Applied Biosystems (Framingham, MA), and calibration protein (aldolase) was obtained from Sigma Proteomass™ kit (Sigma, St. Louis, MO). Trifluoroacetic acid (TFA) was obtained from Pierce (Rockford, IL). Electrophoresis reagents and molecular marker proteins were obtained from BioRad (Hercules, CA). Fluorescent dyes (1-(5-carboxypentyl)-1′-propylindocarbocyanine halide *N*-hydroxy-succinimidyl ester (Cy3) and 1-(5-carboxypentyl)-1′-methylindodi-carbocyanine halide *N*-hydroxysuccinimidyl ester (Cy5)) and immobilized pH gradient (IPG) strips were obtained from Amersham Biosciences (Piscataway, NJ). Protease inhibitors were obtained from either Sigma or Roche. The matrix-assisted laser desorption/ionization (MALDI) matrix, α-cyano-4-hydroxycinnamic acid, and sinapinic acid were purchased from Sigma. All the organic solvents are high-pressure liquid chromatography (HPLC) grade. All other reagents and chemicals were obtained from either Fisher or Sigma and were of the highest purity available.

Parasite Culture and Large-scale Excretory/Secretory Antigen (ESA) Preparation—Parasite culture and ESA preparation was performed according to the protocol described previously (15). Briefly, *T. gondii* strain 2F was propagated in human foreskin fibroblast cells. Freshly egressed tachyzoites, a rapidly dividing parasite stage responsible for acute infection, were harvested by passage twice through a 20-gauge needle followed by filtration through a 3-μm pore size membrane to remove host cell debris. Parasites were washed twice by centrifugation in invasion medium prior to use in experiments. Large-scale preparation of ESA proteins was performed by incubating $\sim 4 \times 10^9$ 2F strain tachyzoites in 15 ml of Dulbecco's modified Eagle's medium (DMEM) containing 2 mM glutamine, 10 mM HEPES, and 1% (v/v) ethanol at 37 °C for 20 min followed by cooling on ice 5 min. Parasites were removed by centrifugation (1000 $\times$ *g*, 10 min, 4 °C), and the supernatant was concentrated to $\sim$400 μl using C-20 concentrators according to the manufacturer's instructions (Millipore, Bedford, MA).

Secretion Experiment and Protease Inhibitor Assay—Tachyzoites (4×10^7/ml) in modified invasion medium (DMEM + 10 mM HEPES) were incubated for 3 min at 37 °C with 1% (v/v) ethanol to stimulate microneme secretion. Tachyzoites were removed by centrifugation (twice at 1000 $\times$ *g*, 10 min, 4 °C), and supernatants were mixed with

Downloaded from http://www.mcponline.org/ by guest on September 22, 2019

SDS-PAGE sample buffer containing 2.0% (v/v) 2-mercaptoethanol for SDS-PAGE and Western blotting (see below). Before being assayed for secretion as described above, tachyzoites were preincubated for 10 min at room temperature with 1% DMSO (solvent control); 1 μM cytochalasin D (CytD); 5 μM pepstatin; 10 mM EDTA (sodium salt); 10 mM EGTA (sodium salt); 5 mM 1,10-phenanthroline; 50 μg ml^{-1} matrix metalloprotease-1 inhibitor; 10 μM 3,4-dichloroisocoumarin; 100 μM L-1-chloro-3-[4-tosylamido]-7-amino-2-heptanone HCl; 100 μM 4-(2-aminoethyl)benzene-sulfonyl)fluoride hydrochloride; 1 mM phenylmethanesulfonyl fluoride (PMSF); 40 μg ml^{-1} leupeptin; 10 μM E-64; and 40 μg ml^{-1} calpain inhibitor I (*N*-acetyl-Leu-Leu-norleucinal (ALLN)) or 40 μg ml^{-1} calpain inhibitor II (*N*-acetyl-Leu-Leu-methioninal (ALLM)).

SDS-PAGE and Western Blotting—Proteins were resolved on 12.5% or 10% reducing SDS-polyacrylamide gels. For Western blotting, PAGE gels were semidry-transferred to nitrocellulose membranes. Blotting was performed as described previously (9) using RαrM2AP (whole serum, 1:5000).

Two-dimensional Gel Electrophoresis (2DE) and Two-dimensional Differential Gel Electrophoresis (2D-DIGE)—ESA proteins were separated in the first dimension using the Ettan IPGphor isoelectric focusing system (Amersham Biosciences). Then 120 μg of ESA protein was mixed with rehydration buffer containing 8 M urea, 2% 3-[(3-cholamidopropyl)dimethylammonio]-1-propanesulfonic acid (CHAPS), 0.5% carrier ampholytes buffer, and 65 mM dithiothreitol (DTT). Rehydration and isoelectric focusing were performed according to the manufacturer's instructions using pH 4–7 IPG strips (13 cm for 2DE, 18 cm for 2D-DIGE). Following isoelectric focusing, proteins were reduced and alkylated by successive 15-min treatments with equilibration buffer containing 2% dithiothreitol followed by 2.5% iodoacetamide. Then, proteins were resolved in the second dimension on a 12.5% SDS-PAGE gel. Resolved proteins were then either transferred directly to PVDF membrane for N-terminal sequencing or stained with colloidal Coomassie Blue stain (21) for MS analysis. 2D-DIGE experiments (22) were carried out as follows: 50 μg lyophilized ALLN-treated and solvent (DMSO) control-treated ESA were each dissolved in 10 μl of labeling buffer (30 mM Tris, 8 M urea, 2% CHAPS, pH 8.5). Then 400 pmol each of Cy3 and Cy5 was added to the ALLN and control samples, respectively, and samples were incubated on ice for 30 min in the dark. After labeling, 1 μl of 10 mM lysine was added to stop the reaction. Cy3- and Cy5-labeled samples were mixed together and resolved by 2DE as described above. Fluorescence scanning was performed using a Typhoon 9200 variable mode imager (Molecular Dynamics, Sunnyvale, CA)

N-terminal Sequencing—Proteins on a 2DE gel were transferred to Immobilon® P^{SQ} membranes (Millipore) and stained with Coomassie Brilliant Blue R-250. Bands were excised and subjected to Edman degradation on a Perkin-Elmer Biosystems Model 477A Gas-Phase Protein Sequencer (Wellesley, MA).

Sequence Analysis—Protein sequence alignments, pI, and molecular mass predictions were performed using Lasergene DNAStar, version 5.00. The web-based programs, ExPASy PeptideMass (ca.expasy.org/tools/peptide-mass.html) and MS-Digest (prospector.ucsf.edu), were also used to predict theoretical molecular mass of protein and peptide digests, respectively.

MALDI Mass Spectrometry—MALDI time-of-flight (TOF) MS was performed using a Voyager DE-STR from PerSeptive Biosystem (Framingham, MA), equipped with a nitrogen laser (337 nm). In all cases unless otherwise specified, spectra were obtained in positive acquisition mode, and external peptides or proteins adjacent to the sample spots were used for MS calibration. Reported peptide masses are monoisotopic, while intact protein masses are average masses.

MALDI-MS Analysis of Intact Protein—Protein bands from 2DE were cut out and solvent-extracted as described (23) with minor modifications. Briefly, excised bands in microtubes were washed with 50 mM ammonium bicarbonate for 10 min, 50% acetonitrile/200 mM NH_4HCO_3 for another 30 min (twice), and finally washed thoroughly with HPLC-grade water. Gel pieces were crushed with a sharp-pointed dental tool. Then 20 μl of 10 mg ml^{-1} sinapinic acid (matrix) in 0.5% TFA/acetonitrile (1:1) was added to cover each gel piece. Samples were extracted by vortexing (moderate speed) at room temperature for 3 h. Following extraction, tubes were opened to evaporate for ~20 min with vortexing until the matrix solution became slightly cloudy, and 1 μl of supernatants were drawn out and deposited onto the MALDI probe for MS analysis. MS spectra were acquired in the linear mode with aldolase as external calibration standard. The mass error of aldolase was less than 10 atomic mass units (amu) after calibration. Acquisition parameters were as follows: acceleration voltage, 25 k; grid voltage, 91%; extraction delay time, 1000 ns; laser shots, 100 per spectrum. The average mass was assigned to each acquired peak in the spectra according to the centroid at 50% height. For assessing experimental deviation, three spectra were acquired for each sample deposited on the plate.

MALDI-MS Analysis of Digested Peptides—Protein spots from PAGE gels were excised, in-gel digested with endoproteinases (12.5 ng μl^{-1} trypsin or 10 ng μl^{-1} Asp-N in 50 mM NH_4HCO_3), and solvent-extracted as described previously (24). Proteins excised from one-dimensional (1D) gels were reduced with DTT (50 mM DTT in 100 mM NH_4CO_3, 56 °C, 1 h) and alkylated with iodoacetamide (275 mM iodoacetamide in 100 mM NH_4CO_3 in the dark at room temperature 45 min) prior to digestion. After extraction, peptide mixtures were dried down and redissolved in 2 μl of 50% acetonitrile and 0.3% TFA, mixed with saturated α-cyano-4-hydroxycinnamic acid (matrix) solution, and deposited on the MALDI-MS target plate according to a general two-layer method (25). The MS spectra were acquired in reflection mode with delayed extraction and were calibrated using calibration peptide mixture II. Peptide mass fingerprints (PMF; a list of highly accurate peptide monoisotopic masses) were used to search against the *Toxoplasma* NCBI database via the MS-Fit algorithm (prospector.ucsf.edu) or searching the FindPept tool (ca.expasy.org/tools/findpept.html). A threshold mass deviation of 50 ppm was used to judge true positive matches in all cases unless otherwise specified.

For in-gel digestion with ^{18}O labeling, digests were performed in 5 mM NH_4HCO_3 with or without the presence of 50% ^{18}O water, using the protease Asp-N at a final concentration of 2 μg ml^{-1}. Digests were acidified and analyzed by MALDI-TOF as previously described (26).

Electrospray Ionization (ESI) Tandem Mass Spectrometry—Peptide sequencing was performed by liquid chromatography tandem MS analysis of peptide fragments from collision-induced dissociation (CID). Peptides were fractionated by reverse-phase HPLC in a 0–60% methanol gradient with 0.5% formic acid over 30 min at ~200 nl min^{-1} on a 75 μm × 100 mm C18 PepMap column using an UltiMate HPLC system, equipped with a FAMOS autoinjector (LC Packings, San Francisco, CA). Eluting peptides were sprayed through a 10-μm picotip (New Objectives, Worburn, MA) directly into a QSTAR Pulsar quadrupole orthogonal TOF tandem mass spectrometer (Applied Biosystems/MDX Sciex, Foster City, CA), equipped with a Protana XYZ manipulator source (MDS Protana A/S, Odense, Denmark). Using the software of Analyst QS (Applied Biosystems), spray, declustering, and focusing potentials were set at 1500, 60, and 220 V, respectively. Peptides were selected for fragmentation in information-dependent acquisition experiments monitoring charge states 2–4 of the two most intense ions. Parent ions were surveyed for 0.5 s, and selected ions were fragmented by CID at 25, 30, and 35 V collision energies. Fragmentation spectra were collected in enhance-all mode over 1.5-s durations. Specific ions of interest were placed in the included list for fragmentation. Errors on fragmentation ions were less than 0.02 amu. The acquired MS data were analyzed with the pro-

Downloaded from http://www.mcponline.org/ by guest on September 22, 2019

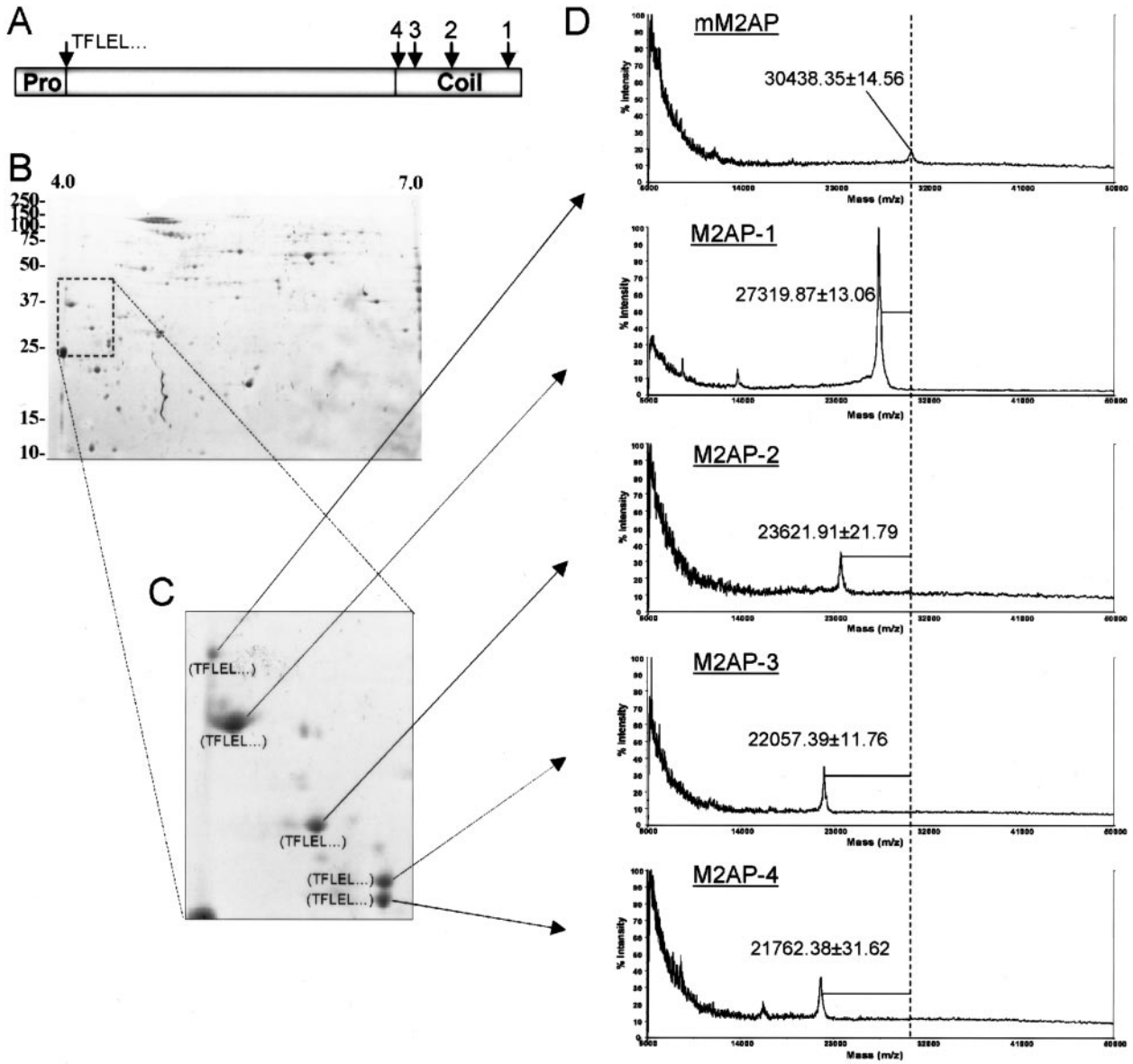

FIG. 1. **MALDI-MS analysis of intact masses of mM2AP and its processing products (M2AP1–4).** *A*, schematic depiction of M2AP showing the propeptide (Pro) cleavage site (*left arrow*), the N-terminal sequence (TFLEL . . .) of the β domain, and approximate positions of processing sites that correspond to M2AP1–4. *B*, coomassie-stained 2DE gel of secretory ESA proteins. Spots corresponding to mM2AP and M2AP1–4 are shown within the *boxed area*. Approximate boundaries of the pH 4.0–7.0 gradient are indicated along the *top* of the gel and positions of molecular mass markers (in kDa) are shown to the *left*. *C*, enlarged region of interest indicating the N-terminal sequences obtained from each spot by Edman degradation. *D*, spots were excised, extracted, and analyzed directly by MALDI-TOF. The average masses of mM2AP and M2AP1–4 are indicated in the respective spectra (indicated peaks correspond to singly charged molecular ions $[M+H]^+$).

grams of Mascot (Matrix Science, London, United Kingdom) or BioAnalyst (Applied Biosystems).

RESULTS

N-terminal Sequencing Reveals C-terminal Proteolysis of M2AP—Proteolytic processing is a common feature for all MICs (8). We previously reported (11) that in addition to the 40-kDa mature M2AP (mM2AP; *i.e.* prodomain removed), a series of four smaller M2AP polypeptides appeared in the ESA fraction. This suggested that mM2AP undergoes proteolytic processing on the surface of the parasite. 2DE of a large-scale ESA preparation confirmed the presence of the four processed products (termed M2AP-1, M2AP-2, M2AP-3, and M2AP-4), which shifted to the alkali end of the first dimension (Fig. 1, *B* and *C*). Based on this shift, we hypothesized that M2AP1–4 were proteolytic products derived from successive proteolysis of the highly acidic C-terminal domain. Confirming this, microsequencing demonstrated that M2AP1–4 each possess the same N terminus (TFLEL . . .) as mM2AP (11).

Downloaded from http://www.mcponline.org/ by guest on September 22, 2019

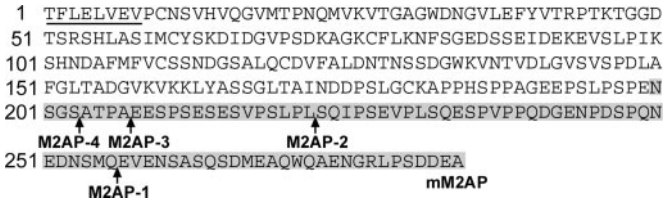

FIG. 2. **Assignment of M2AP C-terminal cleavage sites based on MALDI intact mass.** C-terminal cleavage sites for M2AP1, M2AP2, M2AP3, and M2AP4 are marked with *arrows*. The C-terminal coil domain (aa 200–284) is *shaded*. The N-terminal sequence derived from microsequencing is *underlined*.

Assignment of C-terminal Cleavage Sites of M2AP Based on MALDI Intact Mass Analysis—To determine the precise C-terminal cleavage sites of M2AP processing, we first assigned the cleavage sites on the basis of the intact masses of mM2AP and M2AP1–4. Protein spots corresponding to mM2AP and M2AP1–4 were excised, solvent-extracted, and analyzed by MALDI-TOF. Calibrating with a standard protein (aldolase, 39212.28 average mass) and acquiring MS spectra under parallel acquisition conditions, the masses of mM2AP, M2AP-1, M2AP-2, M2AP-3, and M2AP-4 were measured as 30,438.35, 27,319.87, 23,621.91, 22,057.39, and 21,762.38 Da, respectively (Fig. 1*D*). Because relative mass differences are more accurate than absolute masses, we calculated the sizes of the truncated fragments of M2AP1–4 by subtracting their masses from that of mM2AP. Based on this, we assigned C-terminal cleavage sites for each of the M2AP isoforms (see Fig. 2 and Table I).

Mass Spectrometric Peptide Fingerprints of M2AP1–4 Validates the C-terminal Cleavage Sites—To confirm the M2AP C-terminal cleavage sites, we used specific endoproteinases for in-gel digests of 2DE gel-excised M2AP1–4 spots before acquiring PMFs of the proteolytic digests by MALDI-MS. Tryptic digests of M2AP2–4 in MS spectra revealed peptides with masses that, in every case, closely matched predicted peptide masses corresponding to the cleavage sites defined by intact mass analysis. For example, M2AP-2 showed a peak at *m/z* 4048.677 corresponding to the peptide ^{182}APPHSPPAGEEPSLPSPENSGSATPAEESPSESESVPSLPL^{222} (theoretical *m/z* 4048.879) (Fig. 3*B*). Similarly, for M2AP-3 a prominent peak at *m/z* 2481.044, corresponding to the peptide ^{182}APPHSPPAGEEPSLPSPENSGSATPA^{207} (theoretical *m/z* 2481.153), was observed (Fig. 3*C*). Also, for M2AP-4, a peak at *m/z* 2140.908 closely matched the predicted *m/z*, 2140.978, for the peptide ^{182}APPHSPPAGEEPSLPSPENSGS^{203} (Fig. 3*D*).

However, because of a dearth of basic residues in the C-terminal region of M2AP, tryptic digestion of M2AP-1 was predicted to generate a terminal peptide that would be too large for efficient gel extraction and MALDI analysis (see the sequence in Fig. 2). Accordingly, we failed to identify the M2AP-1 C-terminal peptide in tryptic digests. To obviate this problem, we used endoproteinase Asp-N, which cleaves at the N-terminal side of aspartic acid residues. As shown in Fig. 3*A*, we observed two interesting peaks at *m/z* 595.279 and 611.238 in the Asp-N digest. These peaks are exactly 1 Da larger than the theoretical masses, *m/z* 594.279 and 610.238, of the peptide ^{252}DNSMQ^{256} without and with oxidization of M^{255}, respectively. According to previous studies (27, 28), the 1-Da difference is likely due to deamination of N^{253}. The observation of a parallel addition of 1 Da in its methionine-oxidized derivative strongly supports this interpretation. Collectively, the above data demonstrate that M2AP is processed at highly discrete cleavage sites at Q^{256}/E^{257}, L^{222}/S^{223}, A^{207}/E^{208}, and S^{203}/A^{204}, with the last site corresponding to almost complete removal of the C-terminal coiled domain.

TABLE I
Assignment M2AP C-terminal cleavage sites based on MALDI intact masses

Mature M2AP (mM2AP) and its truncated products (M2AP1–4) were resolved on 2DE gels (Fig. 1, *B* and *C*), excised, and solvent-extracted. Their intact masses were analyzed by MALDI-TOF MS (Fig. 1*D*). The sizes of the truncated fragments of M2AP1–4 were calculated by subtracting their masses from that of mM2AP.

Species	Measured intact mass[a]	Mass difference from mM2AP[b]	Mass deviation (cleavage site)[c]
mM2AP	30,438.35 ± 14.56	0	0
M2AP-1	27,319.87 ± 13.06	3,118.48 ± 26.98	9.34(Q^{256}/E^{257})
M2AP-2	23,621.91 ± 21.79	6,816.44 ± 36.26	31.48(L^{222}/S^{223})
M2AP-3	22,057.39 ± 11.76	8,380.96 ± 24.71	27.34(A^{207}/E^{208})
M2AP-4	21,762.38 ± 31.62	8,675.96 ± 43.23	18.04(S^{203}/A^{204})

[a] Intact mass (± S.D., triplicate measurements) measured by MALDI-TOF MS as described in "Experimental Procedures."

[b] Mass (± S.D., triplicate measurements) difference determined by subtracting the measured intact masses of M2AP1–4 from the measured mass of mM2AP.

[c] Mass deviation from the calculated value based on the cleavage site shown in parentheses.

M2AP Is Processed by Two Distinct Proteolytic Activities—To examine the protease(s) responsible for the surface proteolysis of the M2AP coiled domain, we performed protease inhibitor profiling experiments. As shown in Fig. 4*A*, proteolytic processing of M2AP was affected by a subset of protease inhibitors. These included chymostatin and PMSF, which showed partial inhibition, and the calpain inhibitors ALLN and ALLM, which strongly blocked processing. These inhibitors blocked the formation of the three smallest fragments of M2AP (M2AP2–4), without impairing the two largest fragments (mM2AP and M2AP-1). It should be noted that because the C-terminal coiled domain is highly antigenic, the smaller, more heavily processed species are less well recognized by the antiserum. Therefore, inhibition of M2AP2–4 formation by ALLN and ALLM is more pronounced than indicated by Western blotting. ALLN and ALLM are tripeptide aldehydes previously shown to block removal of an N-terminal extension from MIC2 by MPP2 (15). The following additional evidence further supports that MPP2 is responsible for generating M2AP2–4. First, similar to the observed process-

Downloaded from http://www.mcponline.org/ by guest on September 22, 2019

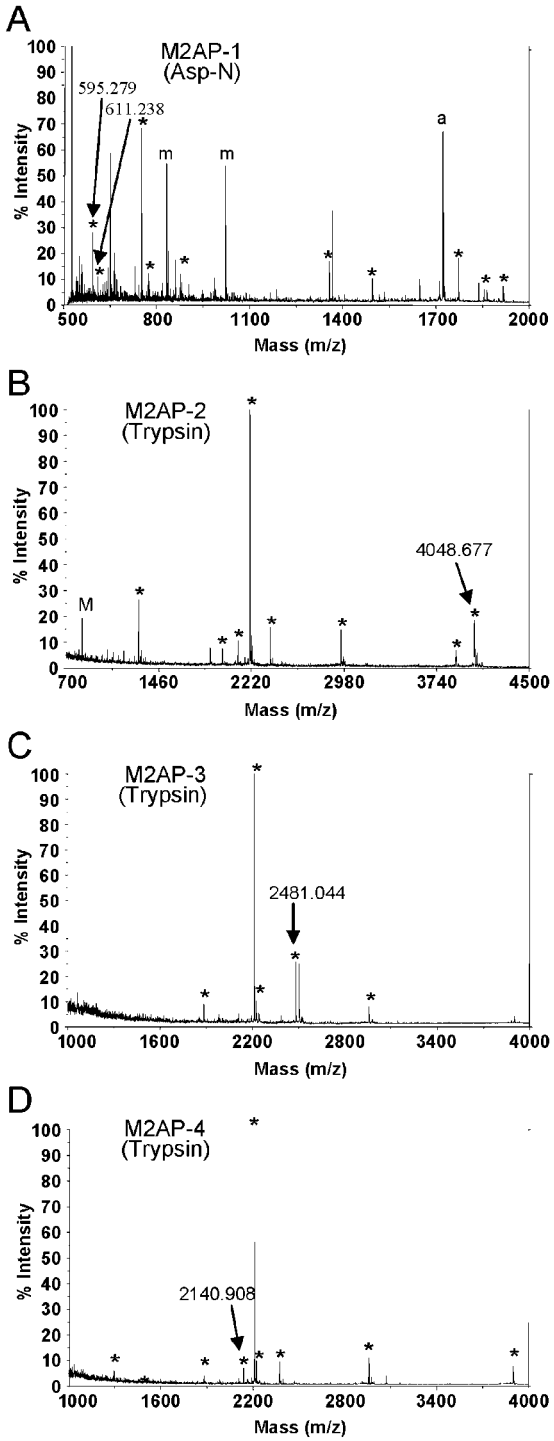

FIG. 3. **MALDI-TOF analysis of M2AP1–4 enzymatic digests.** *A*, Asp-N PMF spectrum of M2AP-1. Ions indicated with *arrows* correspond to deaminated peptides derived from C-terminal cleavage of M2AP-1. a, Asp-N autolysis product; m, matrix ions. *B*, tryptic PMF spectrum of M2AP-2 showing an *m/z* 4048.677 peak corresponding to C-terminal cleavage at M2AP-2. *C*, tryptic PMF spectrum of M2AP-3 revealing an *m/z* 2481.044 peak derived from C-terminal cleavage at M2AP-3. *D*, tryptic PMF spectrum of M2AP-4. The *m/z* 2140.908 peak corresponds to C-terminal cleavage at M2AP-4. Ions marked with an *asterisk* indicate peptides derived from M2AP1–4.

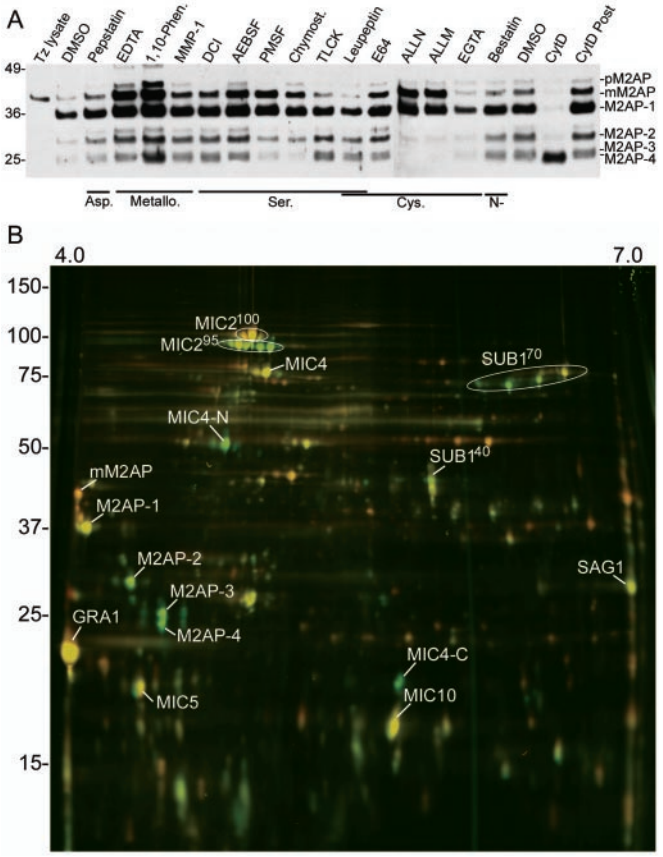

FIG. 4. **Effects of protease inhibitors on proteolytic processing of M2AP.** *A*, ESA samples were prepared from tachyzoites treated with the protease inhibitors indicated at the *top*. Blots were probed with RαrM2AP for detection of M2AP. DMSO, dimethylsulfoxide (solvent control); 1,10-Phen, 1,10-phenanthroline; MMP-1, matrix metalloprotease-1 inhibitor; DCI, dichloroisocoumarin; AEBSF, 4-(2-aminoethyl)benzenesulfonyl)fluoride hydrochloride; PMSF, phenylmethanesulfonyl fluoride; ALLN, *N*-acetyl-leu-leu-norleucinal; ALLM, *N*-acetyl-leu-leu-methioninal; CytD, cytochalasin D; CytD Post, CytD control (CytD was added to the sample just prior to gel-loading to control for a direct effect on migration). *B*, 2D-DIGE analysis ESA proteins collected from parasites treated with DMSO or ALLN were labeled with Cy3 (*green*) or Cy5 (*red*), respectively, and separated by 2DE (pH 4–7 first dimension and 12.5% SDS-PAGE second dimension). Proteins that were diminished by ALLN treatment are *green*. Marked proteins were excised and identified by PMF.

ing of M2AP, trimming of the MIC2 N terminus occurs in multiple steps resulting in removal of a loosely structured region adjacent to a globular domain. Second, M2AP processing is dramatically enhanced by parasite treatment with CytD (Fig. 4*A*), which was previously shown to promote processing by MPP2 (15). Finally, based on processing of MIC2 at V^{50}, G^{66}, and S^{53}, MPP2 prefers to cleave at a small amino acid in the P1 position, which is consistent with the cleavage specificity for M2AP2–4 (L^{222}, A^{207}, and S^{203}, respectively). Although formation of M2AP2–4 appeared to be somewhat sensitive to EGTA, because levels of mM2AP and M2AP-1 were also lower, at least some of this effect is due to inhibition

Downloaded from http://www.mcponline.org/ by guest on September 22, 2019

of microneme secretion, which is calcium dependent.

In contrast to M2AP2–4, formation of M2AP-1 was largely resistant to ALLN and ALLM and instead appeared to accumulate in the presence of these inhibitors. These results suggest that M2AP-1 is generated by a distinct parasite protease we term MPP3. This conclusion is further supported by the observation that the cleavage site specificity (NSMQ/EVEN) of MPP3 is different from that of MPP2. It remains to be determined whether primary cleavage by MPP3 is necessary for subsequent cleavage by MPP2.

In addition to the current findings for M2AP, MPP2 has been previously reported to cleave MIC2 (15) and MIC4 (29). However, it is not known whether MPP2 is exclusively dedicated to these substrates or if it is responsible for processing additional parasite proteins. To globally examine the MPP2 substrate repertoire, we compared ESA proteins from control and ALLN-treated parasites by 2D-DIGE. Control ESA proteins were covalently labeled with Cy3 (pseudocolored green) while ALLN ESA proteins were labeled with Cy5 (pseudocolored red), and the samples were mixed and separated on a single 2D gel. Protein spots that are diminished or absent in the ALLN sample are green, whereas proteins that increase in abundance are red. Spots that do not change significantly are yellow or shades thereof. As expected (Fig. 4*B*), ALLN treatment inhibited the formation of M2AP2–4, MIC2^{95} (product of MPP2's removal of the N-terminal extension), and the MIC4 cleavage products including the ~50-kDa N-terminal product and the "15"-kDa C-terminal product (29). However, ALLN also disrupted processing of SUB1, a microneme subtilase of unknown function, by blocking the formation of several isoforms in the 70-kDa cluster (SUB1^{70}) and the 40-kDa product (SUB1^{40}). Although this implies that MPP2 is responsible for the processing of SUB1, we cannot rule out the possibility that ALLN inhibits other proteases in addition to MPP2. Verification of the complete MPP2 substrate repertoire will require its molecular cloning and the identification of additional selective inhibitors.

MIC2 Is Shed from the Parasite Surface by Intramembrane Cleavage—As mentioned above, recent studies have implied that MIC2 is released from the parasite surface by cleavage within the membrane (20) or outside the membrane (16). To resolve this issue, we purified the secreted form of MIC2 collected from parasite cultures and subjected it to MS analysis by several approaches including PMF analysis, ^{18}O labeling, and tandem MS sequencing.

ESA proteins were resolved by 1D SDS-PAGE, and the band corresponding to MIC2 (indicated in Fig. 5*A*) was excised and subjected to tryptic or Asp-N in-gel digestion. Digests were analyzed by MALDI-TOF, and PMF data were acquired. Analysis of tryptic PMF data confirmed that the excised band was MIC2; however, this data was not suitable for defining the C terminus because trypsin recognizes lysine residues, which potentially constitute the juxtamembrane cleavage site (16). Analysis of the Asp-N spectrum revealed an ion at *m/z* 2748.262 (Fig. 5*B*, *lower spectrum*) corresponding to the peptide ^{678}DENETPTNEEGEQSKKESGSGIAGAIA^{704} (predicted *m/z* 2748.245). This peptide does not have an Asp-N cleavage site at its C terminus, suggesting that it represents the terminal peptide for the shed form of MIC2. Also, this peptide terminates precisely at the intramembrane cleavage site corresponding to that of MIC6 (20) (Fig. 6). In contrast, despite extensive efforts, we did not observe by MALDI-TOF the C-terminal peptide (^{678}DENETPTNEEGEQSK^{692}, theoretical *m/z* 1706.700) representing a juxtamembrane cleavage event at the lysine-containing motif identified by the Sibley group (16).

As an independent method of identifying the C-terminal peptide, we used ^{18}O incorporation to differentially label peptides. As previously described (30), when a protein is digested with a specific protease in the presence of 50% ^{18}O water, the isotopic MS patterns for all newly generated peptides in the spectra are expanded due to the incorporation of one atom of ^{18}O during hydrolysis. Because the original C-terminal peptide in the substrate protein does not undergo cleavage, it fails to incorporate ^{18}O and therefore is the only peptide in the mixture exhibiting a normal isotopic pattern. As shown in Fig. 5*B* (*upper spectrum*), the only unlabeled peak was a signal at *m/z* 2748.262, which corresponds to the same C-terminal peptide identified above (^{678}DENETPTNEEGEQSKKESGSGIAGAIA^{704}). Other peaks all exhibited expanded isotopic patterns (as an example, see inset of magnified spectrum of the peptide ^{288}DGSQIRTRTEVSAPQPGTPTCP^{309} at *m/z* 2355.190).

To unambiguously verify the identity of the C-terminal peptide, we analyzed the Asp-N digests of the shed form of MIC2 with an ESI quadrupole-TOF (QTOF) tandem mass spectrometer. As expected, a triply charged ion ($[M+3H]^{3+}$) with *m/z* 916.7 whose singly charged ion ($[M+H]^{+}$) corresponds to the MALDI ion *m/z* 2748.262 was observed in the ESI-MS spectra. Subsequently, this peptide was selected and fragmented by CID. In the acquired fragmentation spectrum (Fig. 5*C*), the major fragmentation peaks were assigned to "y" and "b" series ions representing truncation from the C and N terminus of the peptide, respectively (fragmentation ions are labeled according to Biemann's nomenclature (31)). Largely based on the assigned "y" series ions (y_1, y_2, y_3, y_4, y_5, y_7, y_8, and y_9; although the y_6 ion was missing, the corresponding b_{22} ion was observed), the partial sequence . . . GSGIAGAIA^{704} was specified, which precisely terminates at the cleavage site identified above. Similarly, the N-terminal sequence ^{678}DENETPTN . . . was largely specified by the "b" series ions in the spectrum (b_2, b_3, b_4, b_5, b_7, b_8; the b_1 and b_6 ions were missing, but the corresponding y_{27} and y_{22} ions were observed). Similar to MALDI-TOF analysis, ESI-QTOF also failed to detect a peptide corresponding to juxtamembrane cleavage at the conserved lysine motif that is necessary for processing.

Based on the above MS evidence, we conclude that MIC2

Downloaded from http://www.mcponline.org/ by guest on September 22, 2019

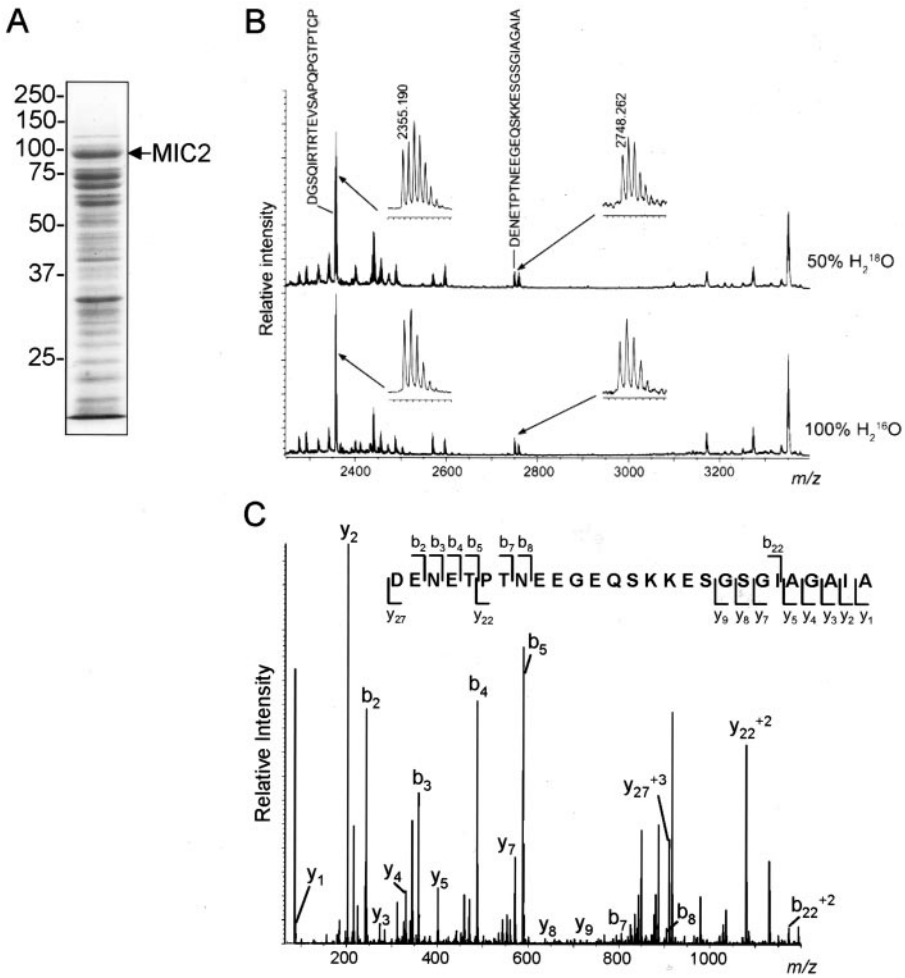

FIG. 5. **Identification of the MIC2 C terminus derived from shedding.** *A*, gel purification of MIC2. ESA proteins were resolved on a 12.5% reducing SDS-PAGE gel and visualized by staining with Coomassie. The band corresponding to MIC2 (*arrow*) was excised and subjected to Asp-N in-gel digestion and extraction. Protein standard markers are shown to the *left*. *B*, partial MALDI-TOF mass spectra of in-gel Asp-N digests of MIC2, performed in the presence of 50% (v/v) ^{18}O water (*upper trace*) or in 100% ^{16}O water (*lower trace*). *Insets* show magnified views of peaks corresponding to peptides ^{288}DGSQIRTRTEVSAPQPGTPTCP^{309} (observed *m/z* 2355.190, predicted *m/z* in carbamidomethylated form 2355.136) and ^{678}DENETPTNEEGEQSKKESGSGIAGAIA^{704} (observed *m/z* 2748.262, predicted *m/z* 2748.245). The latter was the only peptide ion detected that failed to incorporate ^{18}O in digests performed in the presence of ^{18}O, indicating that it derives from the extreme C terminus of the polypeptide substrate. *C*, identification of MIC2 C-terminal peptide in Asp-N digests by ESI tandem MS (MS/MS). After in-gel digestion of MIC2 with Asp-N, peptides were fractionated by reversed-phase HPLC with direct analysis by ESI MS. A triple charged peptide with *m/z* 916.7 was detected, corresponding to the singly charged ion *m/z* 2748.2. Fragmenting the 916.7 peptide generated a partial "y" ion series (y_1, y_2, y_3, y_4, y_5, y_7, y_8, and y_9) representing GSGIAGAIA and a partial "b" ion series representing ENETPTN. These sequences are the C-terminal peptide ^{678}DENETPTNEEGEQSKKESGSGIAGAIA^{704} in the shed form of MIC2.

is shed from the parasite surface by intramembrane proteolytic cleavage at a site near the N-terminal side of its TM anchor. As shown in Fig. 6, alignment of the TM sequences of MIC2 and related proteins reveals that the cleavage site is strikingly well conserved, strongly suggesting that intramembrane cleavage is a general mechanism for shedding adhesive proteins from the surface of apicomplexan parasites.

DISCUSSION

Based on cleavage site specificity and inhibitor profiling data, primary processing of MIC2 and M2AP is mediated by two surface proteases, MPP2 and MPP3. While the detailed properties of these proteases await their molecular cloning and characterization, the available data suggest several clues to their features. First, MPP2 is probably a chymotrypsin-like serine protease or calpain-like cysteine protease based on partial inhibition by chymostatin and PMSF and near complete inhibition by ALLN and ALLM. Because these inhibitors may not be absolutely specific for either class of protease, screening of additional inhibitors will be required to better define the classification of MPP2. Second, we predict that MPP2 resides on the apical surface of the parasite. This is based on the observation that MPP2-mediated processing is dramatically enhanced by treatment with CytD, which dis-

Downloaded from http://www.mcponline.org/ by guest on September 22, 2019

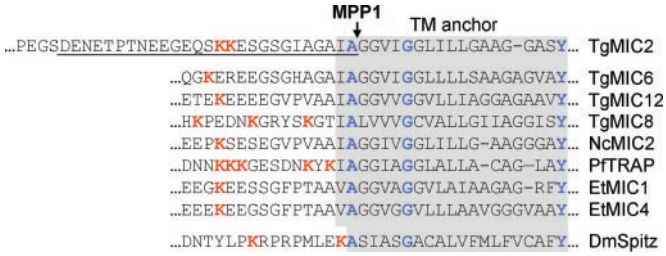

FIG. 6. **The RIP cleavage site for TgMIC2 and related proteins.** Alignment of the juxtamembrane and TM sequences of TgMIC2 and related proteins showing the uniformly conserved amino acids (*blue*) within the TM anchor. Lysine residues implicated in C-terminal cleavage are indicated in *red*. The *underlined* sequence represents the C-terminal peptide derived from N-terminal cleavage by Asp-N and C-terminal cleavage by MPP1. The TM anchor region is highlighted in *gray*.

rupts the actin-dependent redistribution of the MIC2/M2AP complex toward the posterior end of the parasite, effectively trapping the enzyme and substrate together. Finally, MPP2 appears to have a limited substrate repertoire consisting primarily of MIC2, M2AP, MIC4, and SUB1, based on DIGE analysis of the parasite secretory products. While the processing of these substrates appears to be incomplete when assayed using extracellular parasites, it should be noted that in this situation the substrates are probably quickly released from the parasite surface. In contrast, the substrates appear to be stabilized on the parasite surface during invasion (7, 14), presumably leading to more efficient processing.

C-terminal processing of MIC2 by MPP1 is probably a crucial step in invasion based on the finding that parasites expressing a noncleavable copy of MIC2 were significantly impaired in cell entry (16). However, as mentioned above, conflicting evidence regarding the precise cleavage site was reported in two recent studies. Based on biochemical analysis of MIC6 and genetic analysis of MIC2 and MIC12, Soldati and coworkers (20) proposed that MIC2 is cleaved within its TM anchor by regulated intramembrane proteolysis (RIP), a recently identified mechanism of liberating membrane proteins. On the other hand, data reported by Sibley and coworkers (16) suggested that MIC2 is cleaved by juxtamembrane proteolysis (JP) at a dibasic motif consisting of K^{692}/K^{693}, *i.e.* several residues outside the TM anchor. In the present article, we resolve this issue by unequivocally demonstrating that MIC2 is cleaved within its TM anchor at A^{704}/G^{705}. While we cannot completely rule out the possibility of a separate JP cleavage, especially because it has been reported (32, 33) that JP often precedes RIP, we prefer the model that cleavage occurs exclusively by RIP for the following reasons. First, when ALLN or CytD treatment is used to eliminate MIC2 size heterogeneity due to N-terminal processing, MIC2 migrates as a well-defined band, suggesting it is generated by a single cleavage event (15). Second, as exemplified by its similarity to the Rhomboid substrate Spitz (Fig. 6), the MIC2 TM cleavage site closely resembles the recognition sequence for a Rhomboid-like protease (34), which is one of several enzymes capable of mediating RIP. Third, several genes encoding Rhomboid-like proteases are evident in the *Toxoplasma* genome database (D. Soldati, personal communication). Fourth, a recent study demonstrated that *Drosophila* Rhomboid-1 is capable of cleaving a hybrid protein containing the TM region of MIC2 (34). Finally, Rhomboid proteases typically do not require primary processing by JP (32). If indeed MIC2 processing occurs exclusively by RIP, it is possible that the membrane-proximal dibasic motif necessary for MIC2 C-terminal processing is either a distal recognition site for MPP1 (a putative Rhomboid-like protease) or is necessary to maintain the structural integrity of MIC2 for proper intramembrane cleavage.

RIP is generally carried out by multipass membrane proteases and occurs in a wide variety of organisms ranging from bacteria to humans (33). Recently, RIP has gained much attention as a recognized mechanism for intercellular and intracellular signaling (32). It was revealed that RIP mediates important signal transduction events associated with sterol regulation (*e.g.* SREBP cleaved by S2P (35)), cell fate selection (*e.g.* surface receptor Notch cleaved by γ-secretase (36)), and developmental growth regulation (*e.g.* Rhomboid cleavage of the *Drosophila* epidermal growth factor-like membrane proteins Spitz, Keren, and Gurken (37)). Also, the recently identified mammalian signal peptide peptidase is a multipass membrane aspartyl protease responsible for secondary processing of secretory signal peptides (38). In addition, RIP of amyloid precursor protein to produce the amyloid β peptide plays a key role in Alzheimer's disease (39). Despite these established instances, the mechanism of RIP is only beginning to be unveiled, largely because the lipid bilayer presents a challenging experimental environment. Nonetheless, it was recently shown that RIP proteases probably use catalytic mechanisms similar to known proteases that require water to hydrolyze the peptide (32). Given this and considering that TM segments generally adopt a difficult-to-cleave helical conformation, the TM domain of the substrate protein must be at least partially unwound and exposed to the aqueous environment before or during the cleavage to allow water access to the cleavage site buried in the membrane. Accordingly, Urban and Freeman (34) recently suggested that Rhomboid substrates are susceptible to RIP cleavage because their TM domain contains potential helix-breaking residues (*e.g.* G and A), which tend to form a partially disordered conformation. This presumably contributes to the specificity of Rhomboid-like RIP proteases. Our defined RIP cleavage site at A^{704}/G^{705} in the outer portion of the MIC2 membrane segment appears to be consistent with this mechanism for specificity.

Based on the analysis of MIC2/M2AP proteolysis presented herein, we propose a two-step processing model for MIC2/M2AP during invasion (Fig. 7). Once the parasite's apical end attaches to a host cell, the MIC2/M2AP complex is mobilized from the micronemes onto the parasite surface where it un-

Downloaded from http://www.mcponline.org/ by guest on September 22, 2019

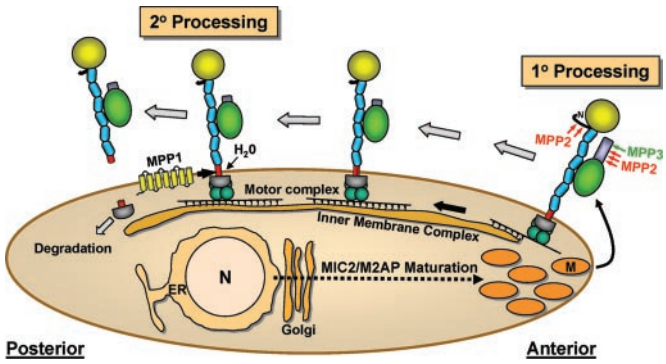

FIG. 7. **A two-step model for proteolytic processing of the MIC2/M2AP complex.** The MIC2/M2AP complex is assembled in the parasite endoplasmic reticulum (*ER*) before undergoing proteolytic maturation to remove a propeptide from M2AP as it transits through the Golgi apparatus en route to the micronemes (*M*). MIC2 is comprised of an N-terminal extension (*N*), which according to the known crystal structures of integrin A-domains probably connects with the base of the MIC2 A-domain (*yellow sphere*). The M-domain (*blue*) of MIC2 likely adopts an extended configuration based on its six subdomains that are similar to thrombospondin type-1 repeats. The TM anchor (*red*) connects the extracellular domains with the C-terminal cytosolic domain. M2AP is comprised of a globular β-domain (*green*) and an extended coiled domain (*purple*). The MIC2/M2AP complex is mobilized from the micronemes to the parasite anterior surface where it engages host receptors during parasite attachment. As the complex is actively translocated by the parasite actin-myosin motility machinery (motor complex) toward the posterior end, MIC2 and M2AP encounter two parasite-derived proteases, MPP2 and MPP3, which remove MIC2's N-terminal extension and M2AP's coiled domain. This primary processing might facilitate interaction with host receptors or clustering of adhesive proteins on the parasite surface. Upon further translocation, the complex undergoes secondary processing by a third parasite protease, MPP1, which is depicted as a multipass integral membrane protein (*yellow cylinders*). RIP cleavage results in shedding of the complex and presumably aids in extracting the C-terminal domain from the membrane to facilitate degradation.

dergoes primary processing by MPP2 and MPP3 at multiple sites (N terminus of MIC2 by MPP2, C terminus of M2AP by MPP2 and MPP3). The role of these primary processing events in invasion remains unknown because the most effective inhibitor of MPP2, ALLN, adversely affects host cells in addition to the parasite (B. F. C. Kafsack and V. B. Carruthers, unpublished observations). Nonetheless, we speculate that primary processing of MIC2/M2AP may facilitate its binding to host receptors or it may activate clustering of the complex with other adhesive proteins at the attachment junction. After primary processing, the receptor-bound complex translocates over the parasite body to the posterior end as the parasite penetrates into the host cell (other MIC adhesins also work in concert here to aid penetration). Upon reaching the extreme posterior end, our data suggests that the complex is disengaged from the parasite surface by MPP1-mediated RIP cleavage within the TM domain of MIC2. If MPP1 is confined to the posterior end of the parasite, this step would be spatially regulated by movement of the substrate into the vicinity of the protease. This type of spatial regulation is commonly associated with RIP (35, 37). However, because the MIC2/M2AP complex is efficiently cleaved by MPP1 in the presence of CytD, at least some MPP1 is likely present on the apical surface. Definitive identification, molecular cloning, and analysis of the MPP1 should help clarify the regulatory mechanism governing the release of adhesive complexes.

RIP cleavage of MIC2 by MPP1 likely fulfills at least four important roles. First, it severs the molecular connection between the parasite and its target host cell, thereby facilitating sealing of the parasitophorous vacuole membrane prior to the completion of cell invasion. Patch clamp studies have shown that this is the slowest, and therefore rate-limiting, step in invasion (40). Second, MPP1 cleavage appears to reduce the affinity of the MIC2/M2AP complex for its receptors (15), thereby preventing retention of the complex on the host plasma membrane after invasion. This probably serves as a mechanism to minimize detection by host immune surveillance. Third, in the absence of host cells, MPP1 cleavage prevents MIC2/M2AP complex from accumulating on the parasite posterior surface. Presumably this is detrimental for invasion because the parasite would then attach to the host cell via its posterior end, thereby precluding correct apical invasion (16). Finally, as suggested by others (33), RIP may facilitate extraction of the C-terminal domain from the membrane for rapid degradation. Indeed, this C-terminal domain appears to be highly unstable because it is undetectable even after maximally stimulating microneme secretion (15). This property likely serves to avoid the C-domain acting as a sink for components of the actin-myosin machinery, which would result in a dominant-negative effect on motility. Because at least MIC2, MIC6, and MIC12 (20) undergo intramembrane cleavage, RIP is likely a general mechanism used by *T. gondii* to shed adhesive proteins during invasion.

Interestingly, proteins on the surface of the malaria merozoite are also subjected to proteolytic processing and shedding during invasion (41). Merozoite surface protein-1 (MSP-1) is initially present as a high-molecular-mass protein expressed on the surface of malaria merozoites and noncovalently complexed with other parasite proteins (41). The 200-kDa MSP-1 precursor is processed into four smaller fragments coincident with merozoite release from an infected cell. During erythrocyte invasion, one of these primary processing products ($MSP\text{-}1_{42}$) is further subjected to a secondary processing, thereby releasing the fragmented MSP-1 ectodomain and its associated partners into the surrounding medium. Only the 19-kDa processed product, $MSP\text{-}1_{19}$, remains on the merozoite surface. The *Plasmodium falciparum* ortholog of AMA1 (PfAMA1) is also shed as a result of juxtamembrane cleavage following its translocation from micronemes onto the merozoite surface (26). Similar to MPP1, the protease responsible for shedding of both these malaria proteins is a membrane-bound enzyme (26, 41). MSP-1 secondary processing has been demonstrated to be essential for successful erythrocyte invasion, and accordingly $MSP\text{-}1_{19}$ is

Downloaded from http://www.mcponline.org/ by guest on September 22, 2019

emerging as a promising target for drug or vaccine development designed to block invasion (42). However, despite the striking similarities between processing of these malaria proteins and MIC2, several important differences exist in their features. First, MSP-1 circumferentially decorates the free merozoite surface, whereas MIC2 is a transient surface protein that is initially deployed only to the parasite apical surface. Second, in contrast to MSP-1, which is "shaved" off the merozoite surface as the moving junction slides over the parasite, MIC2 is excluded by the moving junction, resulting in it being swept toward the posterior end of the parasite during penetration. While some shedding of MIC2 may occur throughout invasion, it appears that much of the surface MIC2 is released from the posterior end of the parasite just prior to completion of invasion (14). Third, and most importantly, shedding of both malaria proteins occurs at JP cleavage sites, whereas secondary processing of MIC2 by MPP1 occurs within the TM anchor by RIP.

In summary, the present study suggests that *T. gondii* uses a dynamic and complex system for processing of MIC proteins during invasion, culminating in the intramembrane cleavage of adhesive complexes from the parasite surface. Given that these proteolytic events are likely crucial for *Toxoplasma* invasion, these findings shed new light on the invasive mechanism of *T. gondii* and provide new insight regarding the properties of parasite proteases that could be attractive therapeutic targets. In addition, these studies provide a novel example of sequential processing associated with RIP-mediated liberation of membrane proteins.

Acknowledgments—We gratefully thank Dr. Robert Cole (Director of the AB Mass Spectrometry Facility at the Johns Hopkins School of Medicine) for invaluable help with some of the mass spectroscopy analysis performed in this study. Funding for the AB Mass Spectrometry Facility at the Johns Hopkins School of Medicine is from a National Center for Research Resources Shared Instrumentation Grant 1S10-RR14702, the Johns Hopkins Fund for Medical Discovery, and the Institute for Cell Engineering. We also thank Claudia Bordon for expert technical assistance, Dominique Soldati for helpful discussions and for generously sharing unpublished observations, and Mae Huynh and Matthew Bogyo for critically reading the manuscript.

* This work is supported by the National Institutes of Health (AI46675; to V. B. C.), the Burroughs Wellcome Fund (to V. B. C.), and the Medical Research Council (to M. J. B.). The costs of publication of this article were defrayed in part by the payment of page charges. This article must therefore be hereby marked "*advertisement*" in accordance with 18 U.S.C. Section 1734 solely to indicate this fact.

¶ To whom correspondence should be addressed: The W. Harry Feinstone Department of Molecular Microbiology and Immunology, Johns Hopkins Bloomberg School of Public Health, 615 N. Wolfe Street, Baltimore, MD 21205. Tel.: 410-614-5592; Fax: 410-955-0105; E-mail address: vcarruth@jhsph.edu.

REFERENCES

1. Jones, J. L., Kruszon-Moran, D., Wilson, M., McQuillan, G., Navin, T., and McAuley, J. B. (2001) Toxoplasma gondii infection in the United States: Seroprevalence and risk factors. *Am. J. Epidemiol.* **154,** 357–365
2. Klemba, M., and Goldberg, D. E. (2002) Biological roles of proteases in parasitic protozoa. *Annu. Rev. Biochem.* **71,** 275–305
3. Shaw, M. K., Roos, D. S., and Tilney, L. G. (2002) Cysteine and serine protease inhibitors block intracellular development and disrupt the secretory pathway of *Toxoplasma gondii*. *Microbes Infect.* **4,** 119–132
4. Conseil, V., Soete, M., and Dubremetz, J. F. (1999) Serine protease inhibitors block invasion of host cells by *Toxoplasma gondii*. *Antimicrob. Agents Chemother.* **43,** 1358–1361
5. Sinai, A. P., and Joiner, K. A. (1997) Safe haven: the cell biology of nonfusogenic pathogen vacuoles. *Annu. Rev. Microbiol.* **51,** 415–462
6. Carruthers, V. B. (1999) Armed and dangerous: *Toxoplasma gondii* uses an arsenal of secretory proteins to infect host cells. *Parasitol. Int.* **48,** 1–10
7. Carruthers, V. B., and Sibley, L. D. (1997) Sequential protein secretion from three distinct organelles of *Toxoplasma gondii* accompanies invasion of human fibroblasts. *Eur. J. Cell Biol.* **73,** 114–123
8. Soldati, D., Dubremetz, J. F., and Lebrun, M. (2001) Microneme proteins: structural and functional requirements to promote adhesion and invasion by the apicomplexan parasite *Toxoplasma gondii*. *Int. J. Parasitol.* **31,** 1293–1302
9. Wan, K. L., Carruthers, V. B., Sibley, L. D., and Ajioka, J. W. (1997) Molecular characterization of an expressed sequence tag locus of *Toxoplasma gondii* encoding the micronemal protein MIC2. *Mol. Biochem. Parasitol.* **84,** 203–214
10. Jewett, T. J., and Sibley, L. D. (2003) Aldolase forms a bridge between cell surface adhesins and the actin cytoskeleton in apicomplexan parasites. *Mol. Cell* **11,** 885–894
11. Rabenau, K. E., Sohrabi, A., Tripathy, A., Reitter, C., Ajioka, J. W., Tomley, F. M., and Carruthers, V. B. (2001) TgM2AP participates in *Toxoplasma gondii* invasion of host cells and is tightly associated with the adhesive protein TgMIC2. *Mol. Microbiol.* **41,** 537–547
12. Morisaki, J. H., Heuser, J. E., and Sibley, L. D. (1995) Invasion of *Toxoplasma gondii* occurs by active penetration of the host cell. *J. Cell Sci.* **108,** 2457–2464
13. Meissner, M., Schluter, D., and Soldati, D. (2002) Role of *Toxoplasma gondii* myosin A in powering parasite gliding and host cell invasion. *Science* **298,** 837–840
14. Carruthers, V. B., Giddings, O. K., and Sibley, L. D. (1999) Secretion of micronemal proteins is associated with *Toxoplasma* invasion of host cells. *Cell. Microbiol.* **1,** 225–235
15. Carruthers, V. B., Sherman, G. D., and Sibley, L. D. (2000) The *Toxoplasma* adhesive protein MIC2 is proteolytically processed at multiple sites by two parasite-derived proteases. *J. Biol. Chem.* **275,** 14346–14353
16. Brossier, F., Jewett, T. J., Lovett, J. L., and Sibley, L. D. (2003) C-terminal processing of the toxoplasma protein MIC2 is essential for invasion into host cells. *J. Biol. Chem.* **278,** 6229–6234
17. Huynh, M. H., Rabenau, K. E., Harper, J. M., Beatty, W. L., Sibley, L. D., and Carruthers, V. B. (2003) Rapid invasion of host cells by Toxoplasma requires secretion of the MIC2-M2AP adhesive protein complex. *EMBO J.* **22,** 2082–2090
18. Donahue, C. G., Carruthers, V. B., Gilk, S. D., and Ward, G. E. (2000) The *Toxoplasma* homolog of *Plasmodium* apical membrane antigen-1 (AMA-1) is a microneme protein secreted in response to elevated intracellular calcium levels. *Mol. Biochem. Parasitol.* **111,** 15–30
19. Cerede, O., Dubremetz, J. F., Bout, D., and Lebrun, M. (2002) The *Toxoplasma gondii* protein MIC3 requires pro-peptide cleavage and dimerization to function as adhesin. *EMBO J.* **21,** 2526–2536
20. Opitz, C., Di Cristina, M., Reiss, M., Ruppert, T., Crisanti, A., and Soldati, D. (2002) Intramembrane cleavage of microneme proteins at the surface of the apicomplexan parasite *Toxoplasma gondii*. *EMBO J.* **21,** 1577–1585
21. Neuhoff, V., Arold, N., Taube, D., and Ehrhardt, W. (1988) Improved staining of proteins in polyacrylamide gels including isoelectric focusing gels with clear background at nanogram sensitivity using Coomassie Brilliant Blue G-250 and R-250. *Electrophoresis* **9,** 255–262
22. Tonge, R., Shaw, J., Middleton, B., Rowlinson, R., Rayner, S., Young, J., Pognan, F., Hawkins, E., Currie, I., and Davison, M. (2001) Validation and development of fluorescence two-dimensional differential gel electrophoresis proteomics technology. *Proteomics* **1,** 377–396
23. Cohen, S. L., and Chait, B. T. (1997) Mass spectrometry of whole proteins eluted from sodium dodecyl sulfate-polyacrylamide gel electrophoresis gels. *Anal. Biochem.* **247,** 257–267
24. Shevchenko, A., Wilm, M., Vorm, O., and Mann, M. (1996) Mass spectro-

Downloaded from http://www.mcponline.org/ by guest on September 22, 2019

metric sequencing of proteins silver-stained polyacrylamide gels. *Anal. Chem.* **68,** 850–858
25. Onnerfjord, P., Ekstrom, S., Bergquist, J., Nilsson, J., Laurell, T., and Marko-Varga, G. (1999) Homogeneous sample preparation for automated high throughput analysis with matrix-assisted laser desorption/ionisation time-of-flight mass spectrometry. *Rapid Commun. Mass Spectrom.* **13,** 315–322
26. Howell, S. A., Well, I., Fleck, S. L., Kettleborough, C., Collins, C. R., and Blackman, M. J. (2003) A single malaria merozoite serine protease mediates shedding of multiple surface proteins by juxtamembrane cleavage. *J. Biol. Chem.* **278,** 23890–23898
27. Wright, H. T. (1991) Nonenzymatic deamidation of asparaginyl and glutaminyl residues in proteins. *Crit. Rev. Biochem. Mol. Biol.* **26,** 1–52
28. Schey, K. L., Little, M., Fowler, J. G., and Crouch, R. K. (2000) Characterization of human lens major intrinsic protein structure. *Invest. Ophthalmol. Vis. Sci.* **41,** 175–182
29. Brecht, S., Carruthers, V. B., Ferguson, D. J., Giddings, O. K., Wang, G., Jaekle, U., Harper, J. M., Sibley, L. D., and Soldati, D. (2001) The *Toxoplasma* micronemal protein MIC4 is an adhesin composed of six conserved apple domains. *J. Biol. Chem.* **276,** 4119–4127
30. Schnolzer, M., Jedrzejewski, P., and Lehmann, W. D. (1996) Protease-catalyzed incorporation of ^{18}O into peptide fragments and its application for protein sequencing by electrospray and matrix-assisted laser desorption/ionization mass spectrometry. *Electrophoresis* **17,** 945–953
31. Biemann, K., and Scoble, H. A. (1987) Characterization by tandem mass spectrometry of structural modifications in proteins. *Science* **237,** 992–998
32. Golde, T. E., and Eckman, C. B. (2003) Physiologic and pathologic events mediated by intramembranous and juxtamembranous proteolysis. *Sci. STKE* **2003,** RE4
33. Brown, M. S., Ye, J., Rawson, R. B., and Goldstein, J. L. (2000) Regulated intramembrane proteolysis: A control mechanism conserved from bacteria to humans. *Cell* **100,** 391–398
34. Urban, S., and Freeman, M. (2003) Substrate specificity of rhomboid intramembrane proteases is governed by helix-breaking residues in the substrate transmembrane domain. *Mol. Cell* **11,** 1425–1434
35. Brown, M. S., and Goldstein, J. L. (1999) A proteolytic pathway that controls the cholesterol content of membranes, cells, and blood. *Proc. Natl. Acad. Sci. U. S. A.* **96,** 11041–11048
36. De Strooper, B., Annaert, W., Cupers, P., Saftig, P., Craessaerts, K., Mumm, J. S., Schroeter, E. H., Schrijvers, V., Wolfe, M. S., Ray, W. J., Goate, A., and Kopan, R. (1999) A presenilin-1-dependent γ-secretase-like protease mediates release of Notch intracellular domain. *Nature* **398,** 518–522
37. Urban, S., Lee, J. R., and Freeman, M. (2002) A family of Rhomboid intramembrane proteases activates all *Drosophila* membrane-tethered EGF ligands. *EMBO J.* **21,** 4277–4286
38. Weihofen, A., Binns, K., Lemberg, M. K., Ashman, K., and Martoglio, B. (2002) Identification of signal peptide peptidase, a presenilin-type aspartic protease. *Science* **296,** 2215–2218
39. Selkoe, D. J. (1996) Amyloid beta-protein and the genetics of Alzheimer's disease. *J. Biol. Chem.* **271,** 18295–18298
40. Suss-Toby, E., Zimmerberg, J., and Ward, G. E. (1996) *Toxoplasma* invasion: The parasitophorous vacuole is formed from host cell plasma membrane and pinches off via a fission pore. *Proc. Natl. Acad. Sci. U. S. A.* **93,** 8413–8418
41. Blackman, M. J. (2000) Proteases involved in erythrocyte invasion by the malaria parasite: Function and potential as chemotherapeutic targets. *Curr. Drug Targets* **1,** 59–83
42. Uthaipibull, C., Aufiero, B., Syed, S. E., Hansen, B., Guevara Patino, J. A., Angov, E., Ling, I. T., Fegeding, K., Morgan, W. D., Ockenhouse, C., Birdsall, B., Feeney, J., Lyon, J. A., and Holder, A. A. (2001) Inhibitory and blocking monoclonal antibody epitopes on merozoite surface protein 1 of the malaria parasite *Plasmodium falciparum*. *J. Mol. Biol.* **307,** 1381–1394

Downloaded from http://www.mcponline.org/ by guest on September 22, 2019